Fabrication of Nanodispersed Pt–Sn/SBA-16 Catalysts and Their Catalytic Applications

Young Kyu Hwang,[1] Deok-Kyu Kim,[1] Ajit Singh Mamman,[1] Sang-Eon Park,[2] and Jong-San Chang*[1]
[1]*Research Center for Nanocatalysts, KRICT, P. O. Box 107, Yuseong, Daejeon 305-600, Korea*
[2]*Department of Chemistry, Inha University, Incheon 402-751, Korea*

(Received September 15, 2006; CL-061079; E-mail: jschang@krict.re.kr)

Monodispersed bimetallic Pt–Sn/SBA-16 catalysts prepared by coimpregnation technique and microwave-drying method showed enhanced catalytic activities for selective dehydrogenation of *n*-dodecane to its corresponding mono-olefins and preferential oxidation (PROX) of CO in the presence of excess H_2.

There has been a considerable interest in preparation, structure and further exploitation of catalytic activity of bimetallic particles ever since Sinfelt[1] demonstrated unique but steady catalytic, reforming properties of alumina-supported Ru–Cu, Pt–Ir, and Pt–Re bimetallic ensembles. Also, highly dispersed platinum and platinum-containing bimetallic catalysts have been extensively studied for industrially important reactions such as dehydrogenation and reforming of hydrocarbon feedstocks[2,3] and preferential oxidation (PROX) of CO in H_2-rich reformate gases.[4,5] Among them, supported bimetallic catalysts such as Pt–Sn alloys are well known as highly versatile catalysts. A concise account of preparation strategies for these catalysts[4,6–8] is described in the literature.

The PROX of CO in a H_2-rich atmosphere has gained tremendous importance because of its application in PEM-FC technology, for its removal from fuel gases produced by reforming processes. The selective dehydrogenation of higher paraffins to the corresponding olefins on supported bimetallic catalysts is also an industrially important process and key step in the manufacture of biodegradable detergents. Highly dispersed, nanostructured bimetallic catalyst encapsulated into SBA-16, to the best of our knowledge and belief, has not been reported so far for these industrially important reactions.

The pure siliceous cubic *Im*3*m* SBA-16 used in the present study was prepared by following the procedure described elsewhere.[9] The reaction solution with molar ratio of $1.0SiO_2$: 3.17×10^{-4}F127:6.68HCl:137.9H_2O was undertaken at 373 K for 24 h. XRD patterns of the calcined SBA-16 showed the well-resolved diffraction peaks indexed to be (100) and (200) support the formation of cubic *Im*3*m* structure of SBA-16 and rule out hexagonal structure. The lattice parameters, $a = 16.2$ nm calculated for the sample were found to be close to the one reported in the literature.[10]

Pt–Sn/SBA-16 catalyst (Figure 1a) was prepared by a simple coimpregnation technique. The known amount of precalcined SBA-16 support ($S_{BET} = 923\,m^2\,g^{-1}$, $V_p = 0.59\,cm^3\,g^{-1}$) was impregnated by using an excess of acidified aqueous solutions of H_2PtCl_6 ($5.13\,mg\,cm^{-3}$) and $SnCl_2$ ($8.42\,mg\,cm^{-3}$) in 10 mL of ethanol. The solution was kept initially in a rotary evaporator at room temperature and finally at 313 K for 2 h in each step. The resultant mass was separately dried in a conventional electric oven at 393 K for 4 h (CE) and in microwave irradiation (MW) for 5 min. Such post-synthetic drying in a microwave drying oven (LG Electronic, 700 W) has numerous advantages[11] over conventional drying. For comparison, metal-loaded samples were dried using conventional electric drying method. The dried samples were subsequently calcined at 773 K for 2 h by increasing the temperature at the rate of $3\,K\,min^{-1}$. The typical composition of the SBA-16 supported catalyst was 1.0 and 2.0% for each of Pt and Sn.

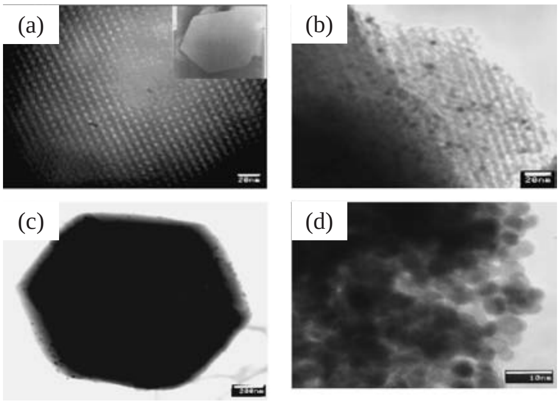

Figure 1. TEM images of SBA-16 and Pt–Sn/SBA-16 prepared by microwave-drying method: (a) calcined SBA-16, (b) 1% Pt–1% Sn/SBA-16, (c) 2% Pt–2% Sn/SBA-16 after H_2 reduction, and (d) Pt–Sn nanoparticles after HF-etching treatment of sample (c).

During synthesis, we observed that the impregnation solution developed dark red color when acidified solution of $SnCl_2$ was added to orange-yellow aqueous solution of acidified H_2PtCl_6. Such change is attributed to the formation of $[Pt(SnCl_3)_2Cl_2]^{2-}$ complex,[12] which is subsequently converted to highly dispersed PtSn alloy particles in the mesopores of SBA-16 substrate when reduced with hydrogen (Figure 1d).

A remarkable decrease in the BET surface area of SBA-16 after its coimpregnation suggests that the Pt–Sn nanoparticles are uniformly dispersed in the mesopores of MW-dried Pt–Sn/SBA-16 catalyst samples (Figures 1b and 1c). Further, etching of 2% Pt–2% Sn/SBA-16 with HF (Figure 1d) shows a crystallographic plane for hexagonal close packing (hcp) bimetallic Pt–Sn alloy particles containing trace amount of face-centered cubic (fcc) $PtSn_2$ phase.[13] As a further evidence, XRD patterns of reduced Pt–Sn/SBA-16 can be indexed as (101), (102), (110), and (202) planes for hcp Pt–Sn structures. However, metallic Sn or $PtSn_2$, if present in traces, may remain undetected.

The dehydrogenation of *n*-dodecane to its corresponding olefin was performed in a continuous flow fixed bed microreactor. The catalyst (1% Sn–1% Pt/SBA-16) was reduced prior to measurement. In a typical experiment, we passed a feed comprising *n*-dodecane and hydrogen (H_2/HC = 6.0, LHSV = $20\,h^{-1}$) over 0.25 g of catalyst packed in a metal reactor at

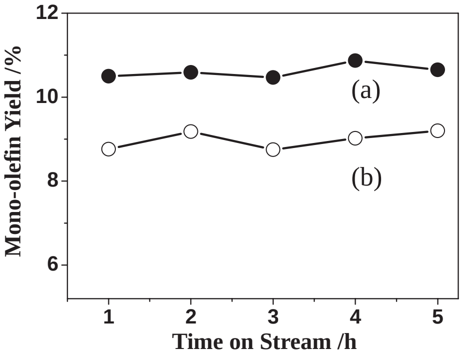

Figure 2. Comparison of mono-olefin yields in dehydrogenation of *n*-dodecane over 1% Pt–1% Sn/SBA-16 catalysts: (a) MW-dried and (b) CE-dried catalysts.

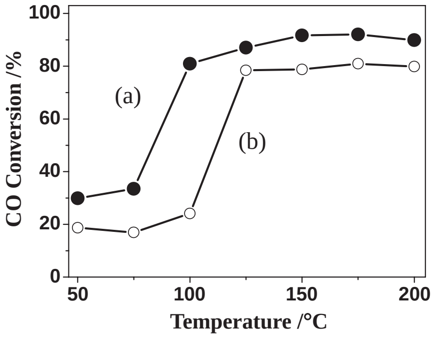

Figure 3. CO conversion for PROX over 2% Pt–2% Sn/SBA-16 in the presence of H_2 as a function of reaction temperature: (a) MW-dried and (b) CE-dried catalysts.

753 K and at atmospheric pressure. The reaction products so formed were analyzed using a Shimadzu liquid chromatograph equipped with a RID-10A refractive index detector. Catalyst performances of MW- and CE-dried Pt–Sn/SBA-16 catalysts for their yields and selectivities for dehydrogenation reaction are compared in Figure 2. It is noted that MW-dried Pt–Sn/SBA-16 shows better catalytic activity (11.1% yield and 90.2% selectivity) than that of CE-dried sample (9.0% yield and 86.1% selectivity) and comparable time-on-stream for 5 h.

Figure 3 shows high CO conversion over 2% Pt–2% Sn/SBA-16 catalysts (MW- and CE-dried samples) under typical reaction conditions. We carried out the PROX of CO by passing a feed comprising mixture of CO/Air/H_2 (1.5/15/120) corresponding to GHSV of $4.2 \times 10^4\,\mathrm{cm^3\,g^{-1}\,h^{-1}}$ over a 0.3 g of catalyst (2% Pt–2% Sn/SBA-16) packed in a continuous flow fixed bed quartz reactor. Prior to evaluating the catalytic activity, the catalyst was prereduced in a flow of 5% H_2 ($100\,\mathrm{mL\,min^{-1}}$) and increasing the temperature at the rate of $3\,\mathrm{K\,min^{-1}}$ and maintaining the final temperature at 673 K for 2 h. The reaction products obtained at different temperatures (50–200 °C) were analyzed by a Chrompack gas chromatograph. It is interesting to note that MW-dried catalyst shows about 93% CO conversion as compared to that 78% for CE-dried one. Also, the CO conversion passes through optimum at 150 °C for both catalysts. This may be attributed to some subtle changes occurring during surface reconstruction. TEM image (Figures 1b and S1) of MW-dried 1% Pt–1% Sn/SBA-16 sample shows uniform dispersion of Pt–Sn particles (3–5 nm) in the mesopores with pore diameter of 5.7 nm of SBA-16 substrate in contrast to CE-dried sample (not shown) after their reduction in flow of 5% H_2. In case of CE-dried sample, Pt–Sn nanoparticles tend to aggregate more at the surface due to slow and nonuniform heating. It is interesting to note that XRD patterns (see Supporting Information) of Pt–Sn/SBA-16 show strong (110) and weak (200) reflections indicating the stability of framework even after coimpregnation of metal components into SBA-16 matrix except that the intensity of first peak is relatively reduced upon increasing the wt % loading.

In summary, the SBA-16, a cubic mesoporous support is successfully used in the present work for encapsulating Pt–Sn nanoparticles. The present study reveals that the Pt–Sn/SBA-16 catalyst unambiguously attains a rather high and uniform dispersion when dried during preparation with microwave irradiation, contrary to its counterpart. Conventional drying results in the peripheral aggregate of the bimetallic alloy particles. Thus, a simple and precise tuning of dispersion can be achieved by MW-irradiation. Such an elegant, cheap and fast technique results in nanostructured Pt–Sn/SBA-16 catalysts which induces a remarkable improvement in the catalytic activity observed for industrially important dehydrogenation of *n*-dodecane and PROX of CO reactions.

This work was supported by the Korea Ministry of Commerce, Industry and Energy (MOCIE) through the Research Center for Nanocatalysts and Institutional Research Progran (KRICT). A. S. Mamman gratefully acknowledges KOFST for awarding Brain Pool fellowship at KRICT.

References and Notes

1 J. H. Sinfelt, *Bimetallic Catalysts: Discoveries, Concepts and Application*, Wiley, New York, **1983**, and references therein; J. H. Sinfelt, *Int. Rev. Phys. Chem.* **1998**, *7*, 281.
2 G. Padmavathi, K. K. Chaudhuri, D. Rajeshwer, G. S. Rao, K. R. Krishnamurthy, P. C. Trivedi, K. K. Hathi, N. Subramanyam, *Chem. Eng. Sci.* **2005**, *60*, 4119.
3 J. D. Cortright, J. A. Dumesic, *J. Catal.* **1995**, *157*, 576.
4 M. M. Schubert, M. J. Kalisch, G. Feldmeyer, M. Huttner, S. Hackenberg, H. A. Gasteiger, R. J. Behm, *Phys. Chem. Chem. Phys.* **2001**, *3*, 1123.
5 A.-Q. Wang, C.-M. Chang, C.-Y. Mou, *J. Phys. Chem. B* **2005**, *109*, 18860.
6 M. C. Roman-Martinez, D. Cazrola-Amoros, H. Yamashita, S. de Miguel, O. A. Scelza, *Langmuir* **2000**, *16*, 1123.
7 R. Morales, L. Melo, A. Llnos, F. Zaera, *J. Mol. Catal. A: Chem.* **2005**, *228*, 227.
8 R. D. Cortright, J. A. Dumesic, *J. Catal.* **1995**, *157*, 576.
9 J. M. Kim, Y. Sakamoto, Y. K. Hwang, Y.-U. Kwon, O. Terasaki, S.-E. Park, G. D. Stucky, *J. Phys. Chem. B* **2002**, *106*, 2552.
10 Y. K. Hwang, J.-S. Chang, Y.-U. Kwon, S.-E. Park, *Microporous Mesoporous Mater.* **2004**, *68*, 21.
11 J. S. Beck, J. C. Vartuli, W. J. Roth, M. E. Leonowicz, C. T. Kresge, T. Schmitt, C. T. W. Chu, D. G. Olson, W. Sheppard, S. B. Mccullen, J. B. Higgins, J. L. J. Schlenker, *J. Am. Chem. Soc.* **1992**, *114*, 10834.
12 R. Srinivasan, L. A. Rice, B. H. Davis, *J. Catal.* **1991**, *129*, 257.
13 G. T. Baronetti, S. R. de Miguel, O. A. Scelza, M. A. Fritzler, A. A. Castro, *Appl. Catal.* **1985**, *19*, 77.

Published on the web (Advance View) December 23, 2006; doi:10.1246/cl.2007.186